EUROPEAN TRANSACTIONS ON ELECTRICAL POWER
Euro. Trans. Electr. Power 2011; **21**:155–164
Published online 21 April 2010 in Wiley Online Library (wileyonlinelibrary.com). DOI: 10.1002/etep.423

RESEARCH ARTICLE

Interpolation approximation of voltage stability constrained opf (vscopf) for reactive power planning

Wenjuan Zhang[1,2], Fangxing Li[1]* and Leon M. Tolbert[1,3]

[1] Department of Electrical Engineering and Computer Science, The University of Tennessee, Knoxville, TN, 37996, U.S.A.
[2] California Independent System Operator, Folsom, CA, U.S.A.
[3] Oak Ridge National Laboratory, Oak Ridge, TN 37831, U.S.A.

ABSTRACT

Reactive power planning (RPP), or Var planning, is to identify the optimal size and location of reactive power sources. In this paper, first, the previous work using least square method to simplify the voltage stability constrained OPF (VSCOPF) model for RPP is presented. Then, this paper presents a new model simplification solution using interpolation. The interpolation approach can be easily applied to a piecewise formulation while preserving the continuity at boundary points, which cannot be easily achieved by previous works like the least square method. The proposed interpolation approach is numerically tested and compared with the least square approach. It is concluded that interpolation is an improved model simplification approach for RPP. Copyright © 2010 John Wiley & Sons, Ltd.

KEYWORDS

voltage stability constrained optimal power flow (VSCOPF); reactive power planning (RPP); total transfer capability (TTC); stability margin (SM); interpolation

***Correspondence**

Fangxing Li, Department of Electrical Engineering and Computer Science, The University of Tennessee; Knoxville, TN 37996, U.S.A.
E-mail: fli6@utk.edu

1. INTRODUCTION

The US power industry has been under great pressure to serve load economically since deregulation was initiated over a decade ago. There has been significant movement towards competitive energy markets. However, reactive power, a critical need for power system operation and planning, has received less attention until most recently due to the Great Northeast Blackout in August 2003. Optimal allocation of Var sources, such as capacitor banks, Static Var Compensators (SVC), and Static Compensators (STATCOM), is a critical component in Reactive Power Planning (RPP), also known as Var planning [1].

Reference [2] demonstrates a technically viable approach to quantitatively assess the benefits from Var sources at the demand side, under the competitive environment. On one hand, injection of reactive power at the receiving end reduces the reactive power through transmission lines, which in turn reduces the line current; thus, the real power loss (I^2R) will also be reduced. In addition, the reduced reactive power flow allows more real power flow if the same MVA capacity is assumed. On the other hand, reactive power compensation can reduce the chance of voltage collapse by increasing the maximum transfer capability or the load level at the point of collapse (PoC), as shown by the three PV curves in Figure 1. It should be noted that a security margin (SM) is typically enforced to ensure that the system is operated with a safe distance from voltage collapse. As shown in Figure 1, SM is measured by the load distance between the operating point, A, and the PoC, B.

Voltage itself is a poor indicator of proximity to system collapse. Thus, the incorporation of voltage stability margin, commonly calculated with continuation power flow (CPF) [3], has become essential when the location and size of new Var sources need to be determined during RPP. The increased total transfer capability (TTC) in Figure 1 due to Var compensation not only pushes the PoC away from the operating point, but helps transfer more lower-cost power to loads. Therefore, the total fuel cost will decrease. The nonlinear relationships exist among the Var compensation, TTC limit, and fuel cost variation, as shown in Figure 2.

Figure 2 also implies a straightforward process to find the optimal Var allocation as described below:

1. For a candidate bus i ($i = 1$ to Last Bus).
2. For a compensation size j ($j = 0$ to Max Size).

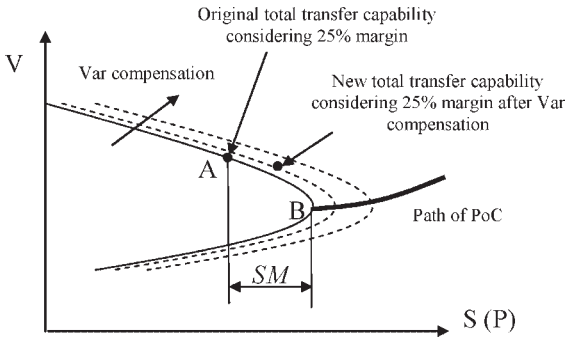

Figure 1. The original and new transfer capability considering security margin.

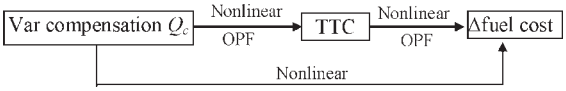

Figure 2. Relationships of fuel cost, TTC, and Var compensation.

3. An optimal power flow (OPF) to maximize TTC is executed to find the new TTC if a *j*-sized Var compensator is connected at the *i*th bus.
4. Another OPF to minimize total cost (fuel cost and Var cost) is executed to determine the changed total cost with the new TTC.
5. Go to Step 2.
6. Go to Step 1.

It should be noted that the two OPF runs in Steps 3 and 4 differ in objective functions while having similar constraints. This process can obtain a set of total cost reduction *versus* Var size curves for different buses, as shown in Figure 3. Certainly, this enumerative approach is straightforward and illustrative for future researchers to simplify models, but very time-consuming since it requires many OPF runs [4,5].

Due to the complicated objective functions and voltage stability constraints discussed previously, RPP is identified as one of the most challenging problems in power systems. Recent research in RPP and related topics has addressed various issues such as incorporation of voltage stability margin [6–9], multi-objective optimization [10–12], intelligent or heuristic searches [13–15], uncertainty factors [16], and pricing of reactive power [17,18]. More references can be found in a detailed literature review [1], which summarizes the three components in optimization-based RPP: the objective function models, the constraint models, and the mathematical algorithms.

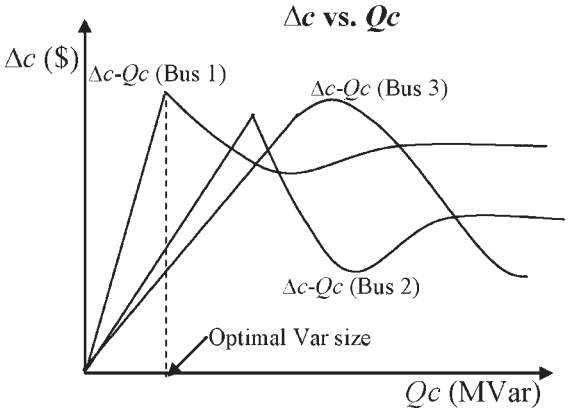

Figure 3. Identify the optimal location and Var size from Δc *versus* Q_c curves.

This paper is organized as follows. Section 2 illustrates the previous work of the least square method for RPP model simplification based on VSCOPF. Section 3 presents the proposed interpolation method for VSCOPF model simplification. Section 4 presents the test results for a seven-bus system with Var compensation. Section 5 presents the conclusion.

2. VSCOPF MODELS WITH LEAST SQUARE APPROXIMATION

As indicated in Reference [8], the major reason for the difficulty in computation and convergence of the complete voltage stability constrained OPF (VSCOPF) model is the requirement of two sets of variables and constraints corresponding to the ''normal operating point ($_o$)'' and ''collapse point ($_*$)''. The two sets of variables become a heavy burden especially for a larger system with many contingency cases. Since each contingency case needs two sets of variables, *n* contingencies need 2*n* sets of variables in the VSCOPF model. The difficulty to converge or find the optimal solution presents a great challenge. Hence, a model simplification may be a welcome addition in cases where the complete VSCOPF model fails to provide any solution due to non-convergence, or it is prone to yield grossly sub-optimal solutions because of its size and complexity.

Reference [8] is a pioneering work that attempts to simplify the VSCOPF RPP model. The simplification is carried out with a linear/quadratic ordinary least-square multivariate regression model to statistically approximate the locus of TTC such that a simple model with lower computational complexity can be obtained. The locus of TTC is estimated using the common TTC OPF approach over various Var compensation scenarios, such as different Var size at each individual bus and various combinations of Var compensation across the buses. The locus of TTC can be expressed as a function of the bus reactive compensation as:

$$\mathrm{TTC} = a + \sum_i b_i Q_{ci} \tag{1}$$

or

$$\mathrm{TTC} = a + \sum_i b_i Q_{ci} + \sum_i c_i Q_{ci}^2 \tag{2}$$

DOI: 10.1002/etep

where a, b_i, and c_i are parameters of the locus which may be estimated using the multivariate ordinary least square (OLS) regression method. However, if the number of candidate buses is increased, the procedure will involve evaluating a large number of Var support configurations to capture the interaction of Var compensation at different locations with specified accuracy.

In addition, the whole RPP model will possibly miss the true optimal solution because the linear and/or quadratic formulations may not have the capability to capture the curve of the TTC *versus* Q_c curve which can be nonlinear or non-quadratic. Thus, a linear or quadratic function, though easier to solve, cannot be used at all in the cases due to losing control of error in a reasonable range. However, piecewise interpolation may create functions suitable for any shape of TTC *versus* Q_c curve with reasonable degree of accuracy as analyzed in the following section.

3. VSCOPF MODEL WITH INTERPOLATION APPROXIMATION

This section proposes the interpolation approximation method to simplify the VSCOPF model, which is an improved approximation model of the previous least square approach.

3.1. VSCOPF model with interpolation approximated total transfer capability (TTC) path function

The analysis explores the possibility to circumvent the two sets of variables, but still incorporate voltage stability constraint such as $\mathrm{SM} \geq \mathrm{SM}_{\mathrm{spec}}$ in the RPP model, by using approximation of the path of TTC, as shown in Figure 1.

In the original VSCOPF model, an additional set of variables is used to indicate the TTC value. If the path of TTC can be approximately estimated beforehand for different Var compensation configurations, this additional set of variables and constraints for TTC state can be eliminated. Based on this idea, the VSCOPF model with TTC *versus* Var function approximated using interpolation is proposed as follows:

$$\mathrm{Min}: \sum f_{1_i}(P_{Gi}) + \sum f_{2_i}(Q_{ci}) \times y_i \tag{3}$$

Subject to:

$$P_{Gi} - P_{Li} - P(V,\theta) = 0 \quad (\text{Real power balance}) \tag{4}$$

$$Q_{Gi} + Q_{ci} - Q_{Li} - Q(V,\theta) = 0 \quad (\text{Reactive power balance}) \tag{5}$$

$$P_{Gi}^{\min} \leq P_{Gi} \leq P_{Gi}^{\max} \quad (\text{Generation real power limits}) \tag{6}$$

$$Q_{Gi}^{\min} \leq Q_{Gi} \leq Q_{Gi}^{\max} \quad (\text{Generation reactive power limits}) \tag{7}$$

$$V_i^{\min} \leq V_i \leq V_i^{\max} \quad (\text{Voltage limits}) \tag{8}$$

$$Q_{ci}^{\min} \leq Q_{ci} \leq Q_{ci}^{\max} \quad (\text{Compensation limits}) \tag{9}$$

$$|\mathrm{LF}_l| \leq \mathrm{LF}_l^{\max} \quad (\text{Line flow thermal limits}) \tag{10}$$

$$\sum_{l \in Lt} \mathrm{LF}_l \leq \mathrm{TTC} \cdot \left(1 - \mathrm{SM}_{\mathrm{spec}}\right) \quad (\text{Tie line transfer limits}) \tag{11}$$

$$\mathrm{TTC} = f(Q_{c1}, Q_{c2}, \ldots, Q_{ck}) \quad (\text{TTC is a function of Var compensation } Q_{ci}) \tag{12}$$

$$\sum y_i = k \quad (\text{Location limit of Var installations}) \tag{13}$$

where

$i \in$ the set of buses; $l \in$ the set of lines;
f_1 —fuel cost function;
f_2 —Var cost function;
P_{Gi} —generator active power output;
Q_{Gi} —generator reactive power output;
P_{Li} —load active power;
Q_{Li} —load reactive power;
Q_{ci} —Var source installed at bus i;
V_i —bus voltage;
LF_l —transmission line flow;
Lt—the set of tie lines;
$\mathrm{SM}_{\mathrm{spec}}$ —specified security margin (such as 25%);
$f(Q_{ci})$—TTC is a function of Q_{ci};
k—the total number of locations to install Var compensators;
y_i —integer variable, ''1'' if there is Var source installed at bus i, otherwise ''0.''

The objective function in Equation (3) considers both the generation cost and the Var cost. This is based on the system operators' viewpoint. As an important transmission level service, Var compensation should be coordinated with generation scheduling. Also, this is feasible since system operators should have a general idea of the network status and market participants. Therefore, it is reasonable to combine generation cost with Var cost in RPP. Certainly, other objective functions (such as minimization of Var cost only) can be employed because of specific requirements and/or constraints in the planning process. Nevertheless, this does not change the key point of this research, which is to provide a new approximation model to include the Var-dependent TTC in RPP.

In general, an interpolation polynomial can estimate the rough shape of a function by using many sampling points. However, this may lead to a high-order polynomial, which is not desired. Fortunately, a piecewise interpolation polynomial algorithm can be adopted such that within each piece, the interpolation polynomial can be kept at an

acceptable order of complexity. Details about generic interpolation and piecewise formulations will be discussed next.

3.2. Lagrange interpolation formula for multi-independent variables on a rectangular grid

For easy visualization, we concentrate on functions of two variables, but extension to more dimensions has no difficulty. Given $(m+1)(n+1)$ interpolation points $(x_i, y_j, z=f(x_i, y_j))$ for the distinct nodes (x_i, y_j), where $i=0, 1,\ldots, m$, $j=0,1,\ldots, n$, we want to find an interpolating algebraic polynomial $p(x, y)$ with $p(x_i, y_j)=f(x_i, y_j)$ for all $i=0,\ldots, m$ and $j=0,\ldots, n$. In general, the existence and uniqueness of an interpolation solution for functions in several variables is not certain. The reason is that if all of the points (x_i, y_j, z_j) lie on a straight line in the $\{x, y, z\}$ space, then there are infinite planes containing this line [19].

However, if specifically the nodes (x_i, y_j) are $(m+1)(n+1)$ distinct points of a rectangular grid, then this special interpolation problem is solvable uniquely in the product form as follows [20]:

$$p(x,y)=\sum_{i=0}^{m}\sum_{j=0}^{n}a_{ij}x^i y^j \tag{14}$$

with $(m+1)(n+1)$ coefficients, a_{ij}, to be determined.

Thus the required polynomial satisfying $p(x_i, y_j)=f(x_i, y_j)$ can be written as [21]

$$p(x,y)=\sum_{i=0}^{m}\sum_{j=0}^{n}f(x_i,y_j)\cdot\prod_{l\neq i}\left(\frac{x-x_l}{x_i-x_l}\right)\cdot\prod_{k\neq j}\left(\frac{y-y_k}{y_j-y_k}\right) \tag{15}$$

3.3. Interpolation error estimation for two variables

Reference [19] indicates that if $f(x)$ has continuous derivatives of orders $m+1$ in the one dimensional interpolation case, then for each $x\in[a, b]$, there exists a point $\xi=\xi(x)$ in the interval $\min(x_0,\ldots,x_m, x)<\xi<\max(x_0,\ldots, x_m, x)$, such that

$$e(x)=f(x)-p(x)=\frac{(x-x_0)(x-x_1)\cdots(x-x_m)}{(m+1)!}f^{(m+1)}(\xi)$$
$$=\frac{\omega_m(x)}{(m+1)!}f^{(m+1)}(\xi)$$

where $\omega_m(x)=\prod_{i=0}^{m}(x-x_i)$ and $e(x)$ is called the error (also called remainder term).

The above equation can be extended to the case of two variables. If $f(x, y)$ has continuous partial derivatives of orders $m+1$ and $n+1$, respectively, in x and y and the appropriate mixed derivative of order $m+n+2$, then by applying the extension of Equation (16), the error/remainder is given by

$$\begin{aligned}e(x,y)&=f(x,y)-p(x,y)\\&=\frac{\omega_m(x)}{(m+1)!}\frac{\partial^{m+1}f(\xi,y)}{\partial x^{m+1}}+\frac{\omega_n(y)}{(n+1)!}\\&\quad\times\frac{\partial^{n+1}f(x,\eta)}{\partial y^{n+1}}-\frac{\omega_m(x)\omega_n(y)}{(m+1)!(n+1)!}\\&\quad\times\frac{\partial^{m+n+2}f(\xi',\eta')}{\partial x^{m+1}\partial y^{n+1}}\end{aligned} \tag{17}$$

where $\omega_n(y)=\prod_{i=0}^{n}(y-y_i)$; ξ and ξ' are in the interval $[\min(x_0,\ldots, x_m, x), \max(x_0,\ldots, x_m, x)]$; and η and η' are in the interval $[\min(y_0,\ldots, y_n, y), \max(y_0,\ldots, y_n, y)]$.

In the case of equidistant nodes and assuming $m=n$, $x_{i+1}=x_i+h$ with $x=x_0+ht_x$ for $t_x\in[0,n]$, and $y_{i+1}=y_i+h$ with $y=y_0+ht_y$ for $t_y\in[0,n]$, we will have special error forms as follows:

$$\begin{aligned}e(x,y)&=\frac{h^{n+1}}{(n+1)!}\left(\pi_n(t_x)\frac{\partial^{n+1}f(\xi,y)}{\partial x^{n+1}}+\pi_n(t_y)\frac{\partial^{n+1}f(x,\eta)}{\partial y^{n+1}}\right)\\&\quad-\frac{h^{2(n+1)}\pi_n(t_x)\pi_n(t_y)}{((n+1)!)^2}\frac{\partial^{2(n+1)}f(\xi',\eta')}{\partial x^{n+1}\partial y^{n+1}}\end{aligned} \tag{18}$$

where h is equidistant along x-axis and y-axis, and $\pi_n(t_x)=\prod_{i=0}^{n}(t_x-i)$; $\pi_n(t_y)=\prod_{i=0}^{n}(t_y-i)$.

Suppose the partial derivatives are all less than M, then the upper bound of error estimation may be derived as follows:

$$|e(x,y)|\leq\left[\frac{h^{n+1}}{(n+1)!}\max|\pi_n(t)|\cdot 2+\left(\frac{h^{n+1}}{(n+1)!}\max|\pi_n(t)|\right)^2\right]\cdot M \tag{19}$$

The partial derivative factor may become large (high degree). Thus, a high degree polynomial interpolation may be risky. To avoid this issue, piecewise-polynomial interpolation is an approach to circumvent the use of high degree polynomial interpolation without abandoning the use of fine grids. Thus, the interpolation of polynomials of high degree can be avoided by partitioning the interval into sufficiently small sub-intervals and interpolating $f(x)$ in each sub-interval by a suitable polynomial [22]. The piecewise interpolation is also helpful to VSCOPF model because higher-order polynomial constraints may cause problems in Nonlinear Programming (NLP).

3.4. Interpolation application procedure

3.4.1. Cutting the feasible region into small sub-regions for piecewise interpolation.

If the degree of polynomial interpolation is fixed as $m=n=3$ in order to be easily solved in VSCOPF model, then it is important to decide the mesh size h that depends on the error estimation. When $n=3$,

$\pi_3(t) = t(t-1)(t-2)(t-3)$, the maximum absolute value of $\pi_3(t)$ is "1" when $t = 0.38$. Substitute $n = 3$ and max $|\pi_3(t)| = 1$ into Equation (18), and Equation (19) is obtained:

$$|e(x,y)| \le \left(\frac{h^4}{12} + \frac{h^8}{24^2}\right) \cdot M \tag{20}$$

If $h = 2$, $|e_n(x, y)| \le 1.78\,M$ (p.u.). If $h = 3$, $|e_n(x, y)| \le 18.14\,M$ (p.u.). If $h = 4$, $|e_n(x, y)| \le 135.11\,M$ (p.u.). This also verifies the higher risk of error if the mesh size grows. With Equation (19), h can be determined based on a desired error threshold and an estimated M, which can be practically evaluated with several sampling points (x_i, y_j).

3.4.2. Piecewise interpolation polynomial functions.

The actual TTC values ($z_{ij} = f(x_i, y_j)$) at the sampling points can be calculated by the common TTC OPF model. Then the points (x_i, y_j, z_{ij}) are interpolated with Equation (15) for two variables on every sub-region. Thus, there is one interpolation polynomial function corresponding to each sub-region. Finally, the overall TTC will have the following format:

$$\mathrm{TTC} = \begin{cases} \mathrm{TTC}_1(x,y) & \text{if}\{a_1 <= x <= b_1, c_1 <= y <= d_1\} \\ \mathrm{TTC}_2(x,y) & \text{if}\{a_2 <= x <= b_2, c_2 <= y <= d_2\} \\ \vdots & \\ \mathrm{TTC}_K(x,y) & \text{if}\{a_K <= x <= b_K, c_K <= y <= d_K\} \end{cases} \tag{21}$$

where a_i, b_i, c_i, and d_i, for $i = 1,\ldots, K$, indicate the boundary of the $K \times K$ sub-regions.

4. CASE STUDY AND RESULTS

4.1. Test system

In this section, the seven-bus test system from PowerWorld [23] is used to demonstrate the optimal location and size selection for Var compensation. The diagram of the test system is shown in Figure 4. The data for the loads, generation, transmission thermal limits, and voltage limits are shown in Table I. In order to study the increased TTC for the tie-line interface (Lines 6-2 and 7-5), the test system is divided into two areas, the Load Center (LC) in the top and the Generation Center (GC) in the bottom, as shown in Figure 4 and Table II. The generators in the LC are more expensive than those in the GC.

The OPF models in this paper are programmed in General Algebraic Modeling System (GAMS), and are solved by the NLP solver MINOS and Mixed Integer Nonlinear Programming (MINLP) solver SBB.

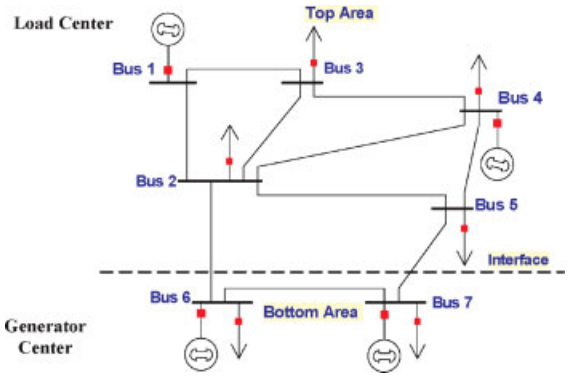

Figure 4. Diagram of a seven-bus test system.

Table I. Parameters of the test system.

Power base: 100MVA							
Voltage base: 138kV							
Load							
Bus	1	2	3	4	5	6	7
P_L (MW)	0	100	190	150	200	50	80
Q_L (MVar)	0	40	75	50	60	20	40
Generator fuel consumption coefficient (Cost = a + b×P_G)							
Bus	1	4	6	7			
a ($/hr)	798.92	814.03	515.34	400.41			
b ($/MWh)	20	19	14	15			
Marginal fuel cost ($/MWh)	20	19	14	15			
Active power generation limits (MW)							
Bus	1	4	6	7			
P_G^{max}	150	200	300	300			
P_G^{min}	70	50	60	0			
Reactive power generation limits (MVar)							
Bus	1	4	6	7			
Q_G^{max}	100	100	100	100			
Q_G^{min}	-100	-100	-100	-100			
Transmission line thermal limits (MVA)							
Line	1-2	1-3	2-3	2-4	2-5	4-3	5-4	6-2	6-7	7-5
Limit	120	100	100	100	100	120	80	250	100	250
Voltage limits (p.u.)										
V_{max} =1.05 and V_{min}=0.95 for every bus.										

4.2. Results from interpolation approximation

To illustrate the results in a three dimensional space for easy visualization, two candidate buses $x = Q_{c3}$ and $y = Q_{c5}$ are chosen. M is estimated using several samples of TTC with different combinations of the two $\{Q_{c3}, Q_{c5}\}$. The mesh size $h = 2$ MVar is preferred based on the error analysis in Section 3 in order to keep the maximum error lower than 1%. The degree of interpolation polynomial is fixed as $m = n = 3$ as introduced in Section 3 to keep the interpolation order low. Then, every sub-region will span

Table II. Load and generation in two areas.

Area	Bus	Gen. Cap. (MW)	Load (MW)	Margin (MW)
Load Center	1, 2, 3, 4, 5	350	640	-290
Gen. Center	6, 7	600	130	470

Table III. TTC values of the sampling points in each sub-region.

Q_{c3} / Q_{c5}	0	2	4	6	8	10	12	...	48
0	4.64	4.66	4.67	4.68	4.69	4.71	4.72		4.83
2	4.68	4.69	4.71	4.72	4.73	4.74	4.76		4.82
4	4.72	4.73	4.75	4.76	4.77	4.78	4.80	...	4.82
6	4.76	4.77	4.79	4.80	4.81	4.82	4.84		4.82
8	4.78	4.81	4.82	4.84	4.85	4.86	4.87		4.81
10	4.84	4.85	4.86	4.88	4.89	4.90	4.90	...	4.81
12	4.88	4.89	4.90	4.92	4.91	4.90	4.90		4.80
14	4.92	4.92	4.92	4.91	4.90	4.90	4.89		4.80
16	4.92	4.92	4.91	4.90	4.90	4.89	4.89	...	4.80
18	4.92	4.91	4.91	4.90	4.89	4.89	4.88		4.79
⋮			⋮			⋮			
48	4.85	4.84	4.84	4.83	4.83	4.83	4.82		4.76

6 MVar along *x*-axis and *y*-axis, respectively. With the assumption that the feasible region is $\{0 \le Q_{c3} \le 48$ MVar, $0 \le Q_{c5} \le 48$ MVar$\}$, the entire region is divided into 64 small pieces by every 6 MVar, such as $\{0 \le Q_{c3} \le 6$, $0 \le Q_{c5} \le 6\}$, $\{6 \le Q_{c3} \le 12$, $0 \le Q_{c5} \le 6\}$, $\{12 \le Q_{c3} \le 18$, $0 \le Q_{c5} \le 6\}$,..., $\{0 \le Q_{c3} \le 6, 6 \le Q_{c5} \le 12\}$, $\{6 \le Q_{c3} \le 12$, $6 \le Q_{c5} \le 12\}$, $\{12 \le Q_{c3} \le 18$, $6 \le Q_{c5} \le 12\}$,..., etc. This is shown in Table III. The cells in gray background are the borders of sub-regions, and the cells in white background are the internal points of each sub-region. Interpolation is applied to every sub-region, thus there will be 64 interpolation functions. The two neighboring interpolation functions will use all the points on their common border, thus all the piecewise functions can be connected continuously such that the overall interpolation is a smooth surface.

The sampling points in Table III are interpolated by using the interpolation formula (15) for two independent variables on every sub-region. All 64 interpolation functions are too long to list, thus only the six TTC approximation functions corresponding to the six sub-regions in Table III are listed in Table IV for illustration. An empty entry in Table IV means that the coefficient is very small and is considered as zero.

Figure 5 shows the original TTC values *versus* two Var sources by step size 1 MVar from the output of the repeated runs of TTC OPF model as a reference for comparison purpose. Figure 6 demonstrates the combination of these piecewise interpolation functions in the whole feasible region. If the sampling step is small enough such as 2 MVar in this case, the maximum error is 0.006 p.u. ($\approx$0.1%), which is apparently acceptable. Certainly, the error will be smaller with a smaller sampling step size if the interpolation polynomial degree is the same.

The result from VSCOPF with interpolation approximation is shown in Table V. The next section will show that the proposed interpolation model may give better results than the least square method presented in the previous work.

4.3. Comparison of interpolation approximation and least square approximation

This subsection compares and discusses the results from the proposed interpolation method and the least square (LS) method presented in Reference [8].

Table VI presents all results from the two model simplification approaches. The results show that the approximation accuracy given in Reference [8] using the least square method can be improved by the proposed piecewise interpolation approximation.

The least square method loses the accuracy on location and size selection, as shown in Table VI. The solution of the least square method gives 25.27 MVar at Bus 5 with calculated TTC (from TTC *versus* Q_c function given by Equation (2)) at 487.20 MVA. As a comparison, the

Table IV. Item coefficients of the sub-interval total transfer capability (*TTC*) interpolation approximation functions ($x = Q_{c3}$, $y = Q_{c5}$).

Func.	TTC_1	TTC_2	TTC_3	TTC_4	TTC_5	TTC_6
x	[0,6]	[6,12]	[12,18]	[0,6]	[6,12]	[12,18]
y	[0,6]	[0,6]	[0,6]	[6,12]	[6,12]	[6,12]
Coefficients of polynomial items						
Const.	4.64	4.64	2.88	4.64	8.35	4.87
x	1.98×10^{-2}	1.98×10^{-2}	3.61×10^{-1}	1.98×10^{-2}	-1.36	1.57×10^{-2}
y	6.28×10^{-3}	6.28×10^{-3}	-1.66	6.28×10^{-3}	-1.57	2.72×10^{-2}
x^2	-1.47×10^{-5}	-1.47×10^{-5}	-2.11×10^{-2}	-1.47×10^{-5}	1.65×10^{-1}	-1.17×10^{-3}
xy			3.43×10^{-1}		5.90×10^{-1}	-5.81×10^{-3}
y^2			6.69×10^{-1}		2.13×10^{-1}	-3.10×10^{-3}
x^3			4.07×10^{-4}		-6.24×10^{-3}	2.47×10^{-5}
x^2y			-2.32×10^{-2}		-7.07×10^{-2}	3.66×10^{-4}
xy^2			-1.35×10^{-1}		-8.00×10^{-2}	5.91×10^{-4}
y^3			-5.58×10^{-2}		-8.89×10^{-3}	1.04×10^{-4}
x^3y			5.13×10^{-4}		2.71×10^{-3}	
x^2y^2			8.91×10^{-3}		9.63×10^{-3}	-3.71×10^{-5}
xy^3			1.12×10^{-2}		3.33×10^{-3}	-1.97×10^{-5}
x^3y^2			-1.94×10^{-4}		-3.70×10^{-4}	
x^2y^3			-7.43×10^{-4}		-4.01×10^{-4}	
x^3y^3			1.62×10^{-5}		1.54×10^{-5}	

DOI: 10.1002/etep

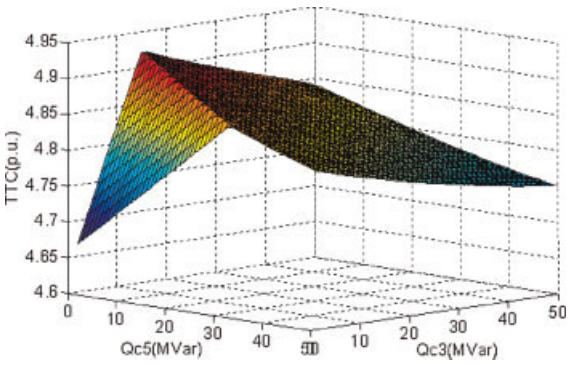

Figure 5. TTC *versus* two Var sources.

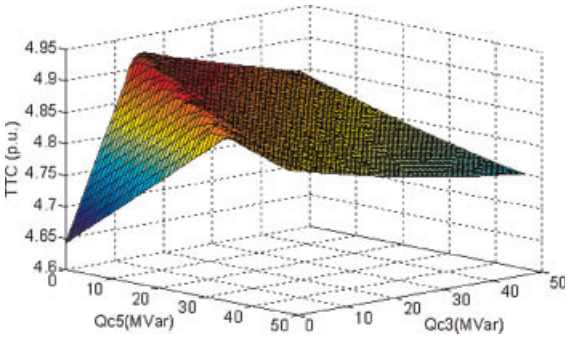

Figure 6. Interpolation approximation of TTC *versus* two Var sources.

Table V. Results from VSCOPF with interpolation approximation.

Objective							
Fuel cost ($/hr)		Var cost ($/hr)			Total cost ($/hr)		
15170.08		25.26			15195.34		
Variables output							
Bus	1	2	3	4	5	6	7
Q_c (MVar)			15.03				
y (binary)			1				
P_G (MW)	85.46			200		300	195.47
Q_G (MVar)	80.46			100		51.58	54.63
P_L (MW)		100	190	150	200	50	80
Q_L (MVar)		40	75	50	60	20	40
V (p.u.)	1.05	1.01	0.99	1.00	0.97	1.04	1.01
TTC (MVA)	492.33						

proposed interpolation method gives 15.03 MVar at Bus 3 with calculated TTC (from piecewise-interpolation TTC *versus* Q_c function in Table IV) at 492.33 MVA. To validate these two methods, the actual TTC is calculated using TTC OPF based on 25.27 MVar at Bus 5 and 15.03 MVar at Bus 3, respectively. This gives 480.18 and 492.56 MVA, respectively. This shows the least square method gives a ''too optimistic'' TTC, while the interpolation method gives a very close result of TTC. Therefore, it is not surprising that the interpolation method generates a very small error in objective function, if the actual TTC is used to re-do the RPP, as shown in the last two rows in Table VI.

It may be misleading when readers observe that the difference of objective functions between two methods ($15242.54 *versus* $15194.54) is very small in percentage. However, this does not mean the insignificance of the proposed method. Two important points should be noted here:

1. The reason of the small error in percentage is that the generation cost to serve the basic system load is very large and essentially independent on Var installation.
2. The actual objective function difference in $ amount is $48/hour (=$15194.54–$15242.54), which is equivalent to $420480/year, a substantial economic difference. This means that the interpolation method gives a result that requires 10.24 MVar (=25.27 − 15.03) less Var compensator, while even producing $420480/year in extra economic gain, if compared with the least square method. This is indeed a significant improvement.

Next, the reason that the least square method does not perform as well as the interpolation method is analyzed. Similar to Reference [8], linear and quadratic function forms are selected here to estimate the TTC function. However, the TTC function loses the accuracy significantly if it is approximated with a quadratic least square function as proposed in Reference [8]. This is shown in Figure 7. The figure shows the TTC approximation using quadratic least square with the assumption that 0–48 MVar is the feasible region and 2 MVar is the step size for sampling points. The least square quadratic polynomial corresponding to Figure 7 is given by

$$\begin{aligned}\mathrm{TTC}|_{(0-50)} &= 4.71 - 1.69 \times 10^{-5} \times Q_{c3}^2 + 1.14 \times 10^{-3} \\ &\quad \times Q_{c3} - 1.56 \times 10^{-4} \times Q_{c5}^2 + 1.02 \times 10^{-2} \\ &\quad \times Q_{c5} \end{aligned} \tag{22}$$

In the above test, both approaches take the same amount of sampling points to approximate the TTC *versus* Var function. This confirms the advantage of the interpolation approach. Or looked at in another way, the interpolation approximation needs less sampling points than the least square approximation for the same accuracy. That is possibly why Reference [8] evaluates many scenarios to obtain a large amount of sampling points. It is important to note that if the least square method is applied to many sub-regions to use a similar piecewise formulation, then the approximated TTC function will not have a continuous boundary between sub-regions in general. This will be problematic, as illustrated by the non-continuous gap at the pre-defined boundary in Figure 8. The reason of the non-continuous gap is that the least square approach will attempt to minimize the average error while not ensuring the exact match of the TTC at the boundary points. As a comparison, since the interpolation approach guarantees the exact match at boundary points, the piecewise interpolation has a continuous TTC function boundary between sub-regions, which is a primary advantage.

Table VI. Comparison of different VSCOPF approaches.

	Least Square Approximation	Interpolation Approximation
Objective ($/hr)	15,217.25	15,195.34
Q_c location	Bus 5	Bus 3
Q_c amount (MVar)	25.27	15.03
Calculated *TTC* (MVA)	487.20	492.33
Actual *TTC*	480.18	492.56
TTC error (MVA)	7.02	0.23
Actual objective ($/hr) based on Actual *TTC*	15,242.54	15,194.54
Actual objective error ($/hr), based on Actual *TTC*	25.29	0.80

Another advantage of the proposed interpolation approach is that it explicitly contains coupling terms such as $Q_{ci} \times Q_{cj}$ corresponding to the interaction of Var compensation at different locations i and j. This is not found in Reference [8]. Instead, Reference [8] considers the coupling effect by using modified values of coefficients b_i and c_i of the linear item Q_{ci} and quadratic item Q_{ci}^2 in Equations (1) and (2). This is also another source of inaccuracy, if compared with the explicit inclusion of the coupling item $Q_{ci} \times Q_{cj}$ in the interpolation method.

The interpolation approach adds approximately 20% increased computational time compared to the least square approach. However, RPP is an off-line planning problem, and the improved accuracy should carry much more weight than the computational time. Therefore, the computational time should not be a concern, while the improvement in solution quality is significant.

Although simulations on larger systems could be even more convincing, the simulation here has presented enough evidence that the proposed interpolation method for VSCOPF model approximation is a useful improvement over the least square approach for model simplification.

5. CONCLUDING REMARKS

In this paper, VSCOPF model for RPP is discussed. The major contribution is the proposed interpolation approach to simplify the transfer capability function with respect to Var sources such that the VSCOPF model for RPP can be simplified. The interpolation model is an improved approach of the least square approximation in the literature because of two reasons:

- Interpolation can be easily expanded to a piecewise function to make a close approximation of any shape, theoretically. However, the least square approach in the previous work cannot handle a shape that is nonlinear and non-quadratic very well, and is not suitable to be modified for a piecewise formulation because that will lead to non-continuous boundary between sub-regions.
- The least square approach proposed in the literature lacks the capability to handle the coupling effect of Var sources at different locations, while the interpolation approach naturally contains coupling items.

It should be noted that the proposed interpolation approximation can be easily applied to a multi-area system with multiple sets of interfaces by modeling the TTC of each interface. In other words, this can be implemented with multiple constraints of Equations (11) and (12). Also, if contingency is considered, only the pre-processing of TTC *versus* Var evaluation needs to be extended to calculate and compare the base case and all credible contingency cases in order to obtain the worst case TTC with respect to

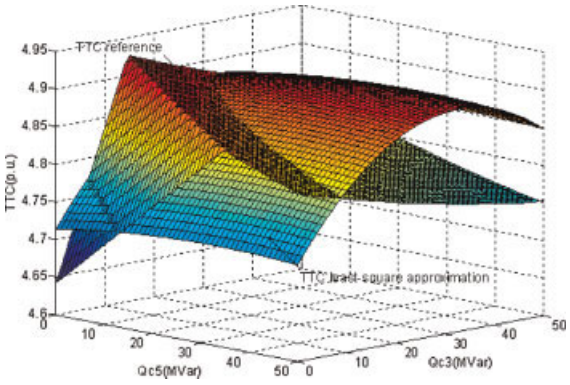

Figure 7. Illustration of TTC approximation error using least square method.

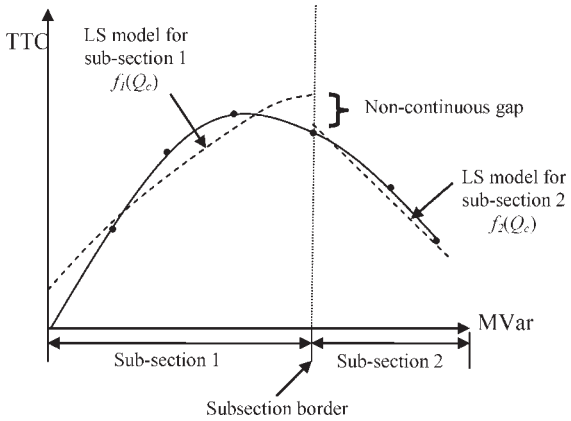

Figure 8. Non-continuous gap at subsection boundary when piecewise least square approximation is applied.

DOI: 10.1002/etep

different possible Var sizes, while the main VSCOPF model in Equations (3)–(13) does not need to be changed.

6. LIST OF ABBREVIATIONS AND SYMBOLS

CPF	continuation power flow
GAMS	general algebraic modeling system
GC	generation center
LC	load center
MINLP	mixed integer nonlinear programming
NLP	nonlinear programming
OLS	ordinary least square
OPF	optimal power flow
PoC	point of collapse
RPP	reactive power planning
SM	stability margin
STATCOM	static compensators
SVC	static Var compensators
TTC	total transfer capability
VSCOPF	voltage stability constrained optimal power flow
a, b_i, and c_i,	parameters of the locus which may be estimated using the multivariate ordinary least square (OLS) regression method
$e(x)$	error (also called remainder term)
h	mesh size
f_1	fuel cost function
f_2	Var cost function
$f(Q_{ci})$	TTC is a function of Q_{ci}
$i\in$	the set of buses
j	compensation size
k	the total number of locations to install Var compensators
$l\in$	the set of lines
LF_l	transmission line flow
Lt	the set of tie lines
m, n	the degree of interpolation polynomial
P_{Gi}	generator active power output
P_{Li}	load active power
$p(x, y)$	interpolating algebraic polynomial
Q_{ci}	Var source installed at bus i
Q_{Gi}	generator reactive power output
Q_{Li}	load reactive power
SM_{spec}	specified security margin (such as 25%)
V_i	bus voltage
y_i	integer variable, ''1'' if there is Var source installed at bus i, otherwise ''0''
^{o}	normal operating point
*	collapse point

ACKNOWLEDGEMENTS

The authors would like to thank the financial support in part by the National Science Foundation under Contract NSF ECS-0093884 and Oak Ridge National Laboratory under Contract 4000041689.

ACKNOWLEDGEMENTS

The authors would like to thank the financial support in part by the National Science Foundation under Contract NSF ECS-0093884 and Oak Ridge National Laboratory under Contract 4000041689.

REFERENCES

1. Zhang W, Li F, Tolbert LM. Review of reactive power planning: objectives, constraints, and algorithms. *IEEE Transactions on Power Systems* 2007; **22**(4): 2177–2186.
2. Li F, Zhang W, Tolbert LM, Kueck JD, Rizy DT. Assessment of the economic benefits from reactive power compensation. *IEEE Power System Conference & Exposition (PSCE 2006)*, Atlanta, GA, October 29–November 01, 2006; 1767–1773.
3. Ajjarapu V, Christy C. The continuation power flow: a tool for steady state voltage stability analysis. *IEEE Transactions on Power Systems* 1992; **7**(1): 416–423.
4. Zhang W, Li F, Tolbert LM. Analysis of Var benefits with application to Var planning. *The 8th International Power Engineering Conference (IPEC 2007)*, Singapore, December 3–6, 2007; 146–152.
5. Zhang W, Li F, Tolbert LM. Voltage stability constrained optimal power flow (VSCOPF) with two sets of variables (TSV) for reactive power planning. *IEEE PES Transmission and Distribution Conference and Exposition (T&D 2008)*, Chicago, April 21–24, 2008.
6. Obadina OO, Berg GJ. Var planning for power system security. *IEEE Transactions on Power Systems* 1989; **4**(2): 677–686.
7. Chattopadhyay D, Chakrabarti BB. Reactive power planning incorporating voltage stability. *International Journal of Electrical Power and Energy Systems* 2002; **24**(3): 185–200.
8. Chattopadhyay D, Chakrabarti BB. Voltage stability constrained Var planning: model simplification using statistical approximation. *International Journal of Electrical Power and Energy Systems* 2001; **23**(5): 349–358.
9. Milano F, Cañizares CA, Ivernizzi M. Voltage stability constrained OPF market models considering N-1 contingency criteria. *Electric Power Systems Research* 2005; **74**(1): 27–36.
10. Hsiao YT, Chiang HD, Liu CC, Chen YL. A computer package for optimal multi-objective VAR planning in large-scale power systems. *IEEE Transactions on Power Systems* 1994; **9**(2): 668–676.
11. Rosehart WD, Cañizares CA, Quintana V. Multi-objective optimal power flows to evaluate voltage security costs in power networks. *IEEE Transactions on Power Systems* 2003; **18**(2): 578–587.
12. He R, Taylor GA, Song YH. Multi-objective optimal reactive power flow including voltage security and demand profile classification. *International Journal of Electrical Power and Energy Systems* 2008; **30**(5): 327–336.

13. Zhu JZ, Chang CS, Yan W, Xu GY. Reactive power optimization using an analytic hierarchical process and a nonlinear optimization neural network approach. *IEE Proceedings — Generation, Transmission, and Distribution* 1998; **145**(1): 89–97.
14. Lee KY, Yang FF. Optimal reactive power planning using evolutionary algorithms: a comparative study for evolutionary programming, evolutionary strategy, genetic algorithm, and linear programming. *IEEE Transactions on Power Systems* 1998; **13**(1): 101–108.
15. Lai LL, Ma JT. New approach of using evolutionary programming to reactive power planning with network contingencies. *European Transactions on Electrical Power* 1997; **7**(3): 211–216.
16. Kim MK, Hur D, Park JK, Yoon YT. Total transfer capability calculation taking into consideration system uncertainties. *European Transactions on Electrical Power* 2009; **19**(1): 72–88.
17. Chattopadhyay D, Bhattacharya K, Parikh J. Optimal reactive power planning and its spot pricing: an integrated approach. *IEEE Transactions on Power Systems* 1995; **10**(4): 2014–2020.
18. El-Samahy I, Bhattacharya K, Caizares C, Anjos MF, Pan J. A procurement market model for reactive power services considering system security. *IEEE Transactions on Power Systems* 2008; **23**(1): 137–149.
19. Isaacson E, Keller HB. Analysis of Numerical Methods. John Wiley & Sons Inc: New York, NY, USA, 1966.
20. Engeln-Müllges G, Uhlig F. Numerical Algorithms with C. Springer Inc.: 1996.
21. Phillips GeorgeM. Interpolation and Approximation by Polynomials. Springer Inc.: 2003.
22. Conte SD, de Boor Carl. Elementary Numerical Analysis: An Algorithmic Approach. McGraw-Hill: 1972.
23. PowerWorld Website,. Accessed on February 2008. http://www.powerworld.com